Received: 5 June 2021 | Revised: 11 August 2021 | Accepted: 12 August 2021

DOI: 10.1096/fba.2021-00067

RESEARCH ARTICLE

FASEB BioAdvances WILEY

CRISPR/Cas9 genome editing reveals an essential role for basigin in maintaining a nonkeratinized squamous epithelium in cornea

Ashley M. Woodward | **Marissa N. Feeley** | **Jamie Rinaldi** | **Pablo Argüeso**

Schepens Eye Research Institute of Massachusetts Eye and Ear, Department of Ophthalmology, Harvard Medical School, Boston, Massachusetts, USA

Correspondence
Pablo Argüeso, Schepens Eye Research Institute of Mass. Eye and Ear, 20 Staniford St., Boston MA 02114, USA.
Email: pablo_argueso@meei.harvard.edu

Funding information
This work was supported by the National Eye Institute, National Institutes of Health, Bethesda, Maryland (grants no.: R01EY024031, R01EY026147, and P30EY003790).

Abstract

One of the primary functions of nonkeratinized stratified squamous epithelia is to protect underlying tissues against chemical, microbial, and mechanical insult. Basigin is a transmembrane matrix metalloproteinase inducer commonly overexpressed during epithelial wound repair and cancer but whose physiological significance in normal epithelial tissue has not been fully explored. Here we used a CRISPR/Cas9 system to study the effect of basigin loss in a human cornea model of squamous epithelial differentiation. We find that epithelial cell cultures lacking basigin change shape and fail to produce a flattened squamous layer on the apical surface. This process is associated with the abnormal expression of the transcription factor SPDEF and the decreased biosynthesis of MUC16 and involucrin necessary for maintaining apical barrier function and structural integrity, respectively. Expression analysis of genes encoding tight junction proteins identified a role for basigin in promoting physiological expression of occludin and members of the claudin family. Functionally, disruption of basigin expression led to increased epithelial cell permeability as evidenced by the decrease in transepithelial electrical resistance and increase in rose bengal flux. Overall, these results suggest that basigin plays a distinct role in maintaining the normal differentiation of stratified squamous human corneal epithelium and could have potential implications to therapies targeting basigin function.

KEYWORDS

basigin, CRISPR/Cas9, human cornea, nonkeratinized squamous epithelium

1 | INTRODUCTION

Nonkeratinized stratified squamous epithelia line the wet surfaces of the cornea, conjunctiva, oral cavity, esophagus, vagina, and ectocervix.[1] This type of epithelium is well suited to resist the abrasive stress that accompanies blinking and the passage of solid food, since superficial cells are constantly desquamating and being replaced before the

Abbreviations: BSA, bovine serum albumin; BSG, basigin; hTCEpi, telomerase-immortalized human corneal epithelial cells; KSFM, keratinocyte serum-free medium; OCT, optimal cutting temperature compound; PAM, protospacer associated motif.

underlying connective tissue is exposed. Similar to other mucosal surfaces, nonkeratinized stratified epithelium is defined by the presence of a mucin coat that provides a protective barrier to pathogens and contribute to lubricate and enhance wettability, thereby preventing desiccation. In addition, the presence of specialized cell–cell and cell–extracellular matrix junctions provide additional barrier functions and play an important role in defining cell morphology and tissue physiology.[2,3]

Basigin (BSG), also known as CD147 or EMMPRIN, is a highly glycosylated transmembrane protein with pleiotropic functions.[4] The human gene, located on chromosome 19, encodes a 269 amino acid protein composed of a 21 amino acid signal sequence, a 186 residue-long extracellular portion with two Ig-like domains, and a highly conserved 21 amino acid transmembrane domain with a 41 residue cytoplasmic tail.[5] Transcription of basigin results in a 29 kDa backbone protein with three asparagine N-glycosylation sites within the Ig-like domains, which can be extended to produce a glycoprotein with a size between 39 and 65 kDa. The pleiotropic nature of this protein is underscored by the diversity of its binding partners. The intramembranous domain of basigin modulates *cis* recognition of numerous molecules within the same membrane, such as members of the monocarboxylate transporter family, GLUT1, and CD44.[6] Basigin also uses its extracellular, glycosylated Ig-like domains to participate in *trans* interactions with opposing cells, resulting not only in the formation of basigin homo-oligomers, but also in the establishment of heterophilic complexes with other molecules such as integrins. These homo- and hetero-interactions influence many biological processes such as cell invasiveness, nutrient transport, and inflammatory signaling pathways. In addition, basigin has also been implicated in facilitating infection by serving as a receptor for viruses such as HSV-1 and, more recently, SARS-CoV-2, responsible for the global pandemic of COVID-19 disease.[7,8]

Basigin was first characterized as a tumor cell-derived collagenase stimulatory factor based on its ability, when expressed on carcinoma cell membranes, to promote MMP-1 biosynthesis by neighboring fibroblasts.[9] Subsequent studies found that basigin has a wider influence in stimulating the biosynthesis of other matrix metalloproteinases, such as gelatinases and stromelysins.[4,10] The use of tissue microarrays has been instrumental in demonstrating that, other than being highly prevalent in human tumors, basigin is present in the normal stratified squamous epithelia of the oral cavity, esophagus, and ectocervix.[11] Basigin has been additionally detected in the stratified squamous epithelium of the human cornea, although its expression dramatically increases in several pathological states including ulceration, dry eye, and keratoconus.[12-15] The excessive degradation of cellular junctions and extracellular matrix that follows the upregulation of basigin in pathological states has been primarily associated with the induction of matrix metalloproteinase activity. Consequently, repressing basigin expression or function has been proposed as a therapeutic modality, yet the adverse implications of this approach to physiological processes remain a concern.[11,16] Here, we took advantage of a CRISPR/Cas9 genome editing approach to determine whether homeostatic expression of basigin contributes to maintain human corneal epithelial integrity. We find that basigin plays an essential role sustaining the structure and normal differentiation of stratified squamous cells and promoting epithelial barrier function.

2 | MATERIALS AND METHODS

2.1 | Cell culture and human tissue

The telomerase-immortalized human corneal epithelial cell line, hTCEpi, was used in this study. These cells stratify, differentiate, and desquamate similar to normal human corneal epithelium.[17] For the establishment of multilayered cell cultures, cells were plated at a seeding density of 4×10^5 cells/cm^2 and maintained in keratinocyte serum-free medium (KSFM; Thermo Fisher Scientific) until confluence. Thereafter, cells were grown in DMEM/Ham's F-12 media supplemented with 10% newborn calf serum and 10 ng/ml epidermal growth factor for 7 days to promote stratification and differentiation. Healthy human corneal epithelial tissue was collected from donors who underwent LASIK surgery under an Institutional Review Board-approved protocol for discarded tissue and frozen in optimal cutting temperature compound (OCT).

2.2 | CRISPR/Cas9-mediated gene editing

LentiCRISPRv2GFP, an all-in-one lentiviral-delivery system containing an eGFP fluorescent reporter, Cas9 enzyme and single guide RNA (sgRNA) scaffold, was a gift from David Feldser (Addgene plasmid #82416).[18] Three sgRNAs containing a 20-nucleotide sequence targeting basigin and an NGG protospacer associated motif (PAM) sequence were designed using the CRISPR Design Tool (http://crispr.mit.edu/) to minimize off-target effects (Table S1). The sgRNAs were annealed and cloned into LentiCRISPRv2GFP vector by digestion with Esp3I (Thermo Scientific). The ligated products were transformed into NEB Stable Competent *E. coli* via heat-shock and single colonies were used for plasmid preparation (QIAprep Spin Miniprep Kit; Qiagen). Plasmids from

single colonies were sequenced to confirm integration of the sgRNAs into the LentiCRISPRv2GFP vector.

The sequence-verified constructs were transfected into mammalian cells using a standard transfection protocol.[19] Briefly, HEK 293T cells were transfected with LentiCRISPRv2GFP+sgRNA, the packaging plasmid psPAX2 (gift from Didier Trono; Addgene plasmid # 12260) and the envelop plasmid pCMV-VSV-G (gift from Bob Weinberg; Addgene plasmid # 8454) in the presence of polyethylenimine (Sigma-Aldrich) in serum-free DMEM. Media was changed to DMEM with 10% fetal bovine serum at 6 hours post-transfection and the viral particle-containing media was collected at 24, 48, and 72 hours. The lentivirus preparations were titrated using the qPCR Lentivirus Titration Kit (Applied Biological Materials).

For transduction of hTCEpi cells, 3×10^5 cells per well were plated in 6-well plates and infected 24 hours later at a MOI of 25 or 50. Normal growth medium was removed before adding 2 ml inoculation medium containing the lentivirus and 8 μg/ml polybrene transfection reagent (Sigma-Aldrich). The lentivirus was omitted in noninfected controls. The culture medium was changed 24 hours later to KSFM alone. Approximately 14 days post-infection, cells were stained with PE-conjugated mouse anti-human basigin antibody (1:200; 8D12; Thermo Fisher Scientific) in 2% fetal calf serum for 45 minutes on ice in the dark. Cells were then washed and resuspended in FACS sorting buffer (1 mM EDTA, 25 mM HEPES pH 7.0, 1% heat-inactivated FBS and 5 units/ml DNAse in PBS). Subpopulations of GFP^+BSG^- cell suspensions were separated on a FACSAria Fusion Cell Sorter (BD Biosciences) and collected in KSFM containing 1% penicillin/streptomycin and 20% FBS. Noninfected cells were stained with PE-basigin antibody and used as gating controls. Basigin KO single cell clones were grown subsequently to prevent allelic heterogeneity. Sorted cells were diluted in KSFM to a concentration of 5 cells/ml. Then, 200 μl cell suspensions were added to each well of a 96-well plate and cells were cultured for 10–14 days before expansion. Knockout efficiency was assessed by immunoblotting for basigin. sgRNA-3 produced a clone with undetectable levels of basigin and was used in further experiments. The Cas-OFFinder algorithm was used to identify potential off-target sites with up to three mismatches, by comparing the sgRNA target site for basigin against the *Homo sapiens* GRCh38/hg38 reference genome.[20]

2.3 | Histology and scanning electron microscopy

Histological assessment was carried out in cell cultures grown on 12-well Transwell inserts (Corning). The samples were fixed with half strength Karnovsky's fixative, post-fixed in 2% osmium tetroxide, dehydrated with graded ethyl alcohol solutions and embedded in tEPON-812 epoxy resin (Tousimis) in a Llynx II EM Tissue Processor (Electron Microscopy Sciences). Semi-thin (1 μm) sections were cut on a Leica EM UC7 ultramicrotome (Leica Microsystems), stained with toluidine blue and imaged by brightfield microscopy. For scanning electron microscopy, cell cultures were grown on 12 mm diameter glass coverslips, fixed in half strength Karnovsky's fixative, dehydrated through an ethanol series, critical point dried with a SamDri-795 critical point dryer (Tousimis) and coated with chromium using an Ion Beam Coater 610 (Gatan). Samples were photographed on a JEOL 7401F Field Emission scanning electron microscope (JEOL). The area of cells with unambiguous cell–cell borders was outlined and quantified using ImageJ software (National Institutes of Health).

2.4 | Immunofluorescence

OCT-embedded human corneal specimens were cut in 10-μm sections and placed onto glass slides. Sections were fixed in methanol at −20°C for 10 minutes, rehydrated with PBS and incubated with 3% bovine serum albumin (BSA) in PBS for 10 minutes. Slides were incubated overnight with mouse anti-human basigin (1:100; clone HIM6; BioLegend) or isotype control antibody in 1% BSA in PBS. Samples were treated with Alexa Fluor 488 rabbit anti-mouse IgG antibody (1:500) for 1 hour at room temperature. Cell cultures grown on 8-well chamber slides were fixed in 4% paraformaldehyde for 20 minutes, permeabilized with 0.25% Triton-X 100 in PBS for 10 minutes (for ZO-1 and occludin) and blocked with 3% BSA in PBS for 30 minutes at room temperature. Slides were then incubated with rabbit anti-ZO-1 (1:150; 61–7300; Thermo Fisher Scientific), mouse anti-occludin (1:150; OC-3F10; Thermo Fisher Scientific), mouse anti-MUC16 (1:300; M11; Neomarkers), or isotype control antibody overnight on a shaker at 4°C, followed by incubation with AlexaFluor 488 goat anti-rabbit IgG (1:50 for ZO-1) or goat anti-mouse IgG (1:300 for occludin; 1:100 for MUC16) antibody for 2 hours at room temperature. Cells were washed twice for 5 minutes in PBS between each step. Nuclei were counterstained using Vectashield with DAPI (Vector Laboratories). To determine cell area, the cell–cell border area in each image was outlined using ZO-1 staining and quantified using ImageJ software (National Institutes of Health).

2.5 | Immunoblotting

Cells were lysed in RIPA buffer supplemented with cOmplete EDTA-free Protease Inhibitor Cocktail (Roche Diagnostics).

After homogenization with a pellet pestle, cell extracts were centrifuged at 17,115 *g* for 45 minutes at 4°C, and the protein concentration of the supernatant determined using the Pierce BCA Protein Assay Kit (Thermo Fisher Scientific). Proteins were separated by SDS-PAGE (10 or 15% resolving gel) and electroblotted onto nitrocellulose membranes. For MUC16 detection, proteins were separated by 1% agarose gel electrophoresis and blotted onto nitrocellulose membranes using vacuum. Nonspecific binding to the nitrocellulose was blocked by incubation with 5% nonfat milk in Tris-buffered saline with 0.1% Tween 20 at room temperature for 1 hour. Membranes were then incubated with primary antibodies to basigin (1:3,000; A12; Santa Cruz Biotechnology), NCOR2 (1:250; PA1-843; Thermo Fisher Scientific), MUC16 (1:3,000; M11; Thermo Fisher Scientific), MUC1 (1:3,000; 214D4; EMD Millipore), involucrin (1:1,000; SY5; Thermo Fisher Scientific), galectin-3 (1:3,000; H160; Santa Cruz Biotechnology), occludin (1:1,000; OC-3F10; Thermo Fisher Scientific), or claudin-4 (1:300; 3E2C1, Thermo Fisher Scientific) in blocking buffer overnight at 4°C. GAPDH (1:3,000; FL-335; Santa Cruz Biotechnology) staining served as a sample loading control. Membranes were then incubated with the appropriate secondary antibodies coupled to horseradish peroxidase (1:3,000; Santa Cruz Biotechnology) for 1 hour at room temperature. Peroxidase activity was visualized using chemiluminescence. Densitometry was performed using ImageJ software.

2.6 | Zymography

Cell culture medium was collected and centrifuged at 21,130 *g* for 5 minutes to remove cells and cellular debris. The supernatant (30 μl) was mixed with nonreducing loading buffer (50 mM Tris-HCl pH 6.8, 10% glycerol, 1% SDS, and 0.01% bromophenol blue) and resolved on 7.5% SDS-PAGE gels containing 1 mg/ml gelatin (bovine skin type B). Gels were then incubated in 50 mM Tris containing 5 mM $CaCl_2$, and 2.5% Triton-X 100 for 2 hours at room temperature. After washing with distilled water, gels were incubated in collagenase buffer (50 mM Tris-HCl pH 7.6, 5 mM $CaCl_2$) for 24 hours at 37°C followed by staining in Coomassie Brilliant Blue solution (40% methanol, 10% acetic acid, 0.025% Coomassie Brilliant Blue R-250) for 2 hours at room temperature. Gels were then washed in distilled water, destained with 40% methanol and 10% acetic acid for at least 1 hour and photographed. Gelatinase activity was quantified using ImageJ software.

2.7 | MTS assay

MTS assay was performed using the CellTiter 96 AQ_{ueous} One Solution Cell Proliferation Assay (Promega). Here, cells were seeded onto 12-well plates (4×10^5 cells/well) and switched to stratification medium upon confluence for the indicated lengths of time. Subsequently, the cells were incubated with AQ_{ueous} One Solution Reagent mixed with stratification medium (1:5, vol:vol) for 1 hour at 37°C in 5% CO_2. The medium was transferred to a 96-well plate in triplicate and the absorbance read at 495 nm.

2.8 | qPCR and human tight junction PCR array

Total RNA was extracted from cell cultures using the RNeasy Plus Mini Kit (Qiagen). Up to 1 μg total RNA was used for cDNA synthesis (RT^2 First Strand Kit; Qiagen). Gene expression levels were detected by qPCR using the SYBR Fast qPCR kit (Kapa Biosystems) in a Mastercycler ep realplex thermal cycler (Eppendorf). Primer sequences for *SPDEF*, *KLF4*, and *GAPDH* were obtained from Bio-Rad (catalog numbers qHsaCID0021209, qHsaCED0044721, and qHsaCED0038674, respectively). Primer sequences for *ELF3* have been previously published.[21] All qPCR samples were normalized using *GAPDH* housekeeping gene expression. The expression of 84 genes associated with tight junctions was evaluated using a human RT^2 Profiler PCR array (PAHS-143Z; Qiagen) according to the manufacturer's instructions. The array was repeated twice with independently isolated RNA. Expression values were normalized by automatic selection of an optimal set of reference genes. The $\Delta\Delta C_T$ and ΔC_T methods were used for relative quantification of the number of transcripts.

2.9 | Barrier function

Transcellular barrier function was assayed with the rose bengal anionic dye as previously described.[22] Cells in tissue culture plates were rinsed with PBS and incubated for 5 minutes with a 0.1% solution of rose bengal (Acros Organics) in PBS. Afterwards, the dye was aspirated and the culture washed with PBS. The extent of dye penetrance was assessed using an inverted microscope (Nikon Eclipse TS100). Images were taken at 20× magnification with a SPOT Insight Fire Wire Camera (Diagnostic Instruments) and analyzed using ImageJ software. Transepithelial electrical resistance was determined on cells grown in Transwell cell culture inserts using an EVOM2 Epithelial Voltohmmeter (World Precision Instruments). Before each measurement, the voltohmmeter was "zeroed" according to the manufacturer's instructions. One Transwell insert was left empty as a control to determine the intrinsic resistance of the filter, which was subtracted from all readings. Transepithelial resistance (ohm-square centimeters)

was calculated by multiplying the measured electrical resistance by the area of the filter (1.12 cm^2).

2.10 | Statistical analysis

Statistical analyses were performed using Prism software version 7 (GraphPad Software).

3 | RESULTS

3.1 | Loss of basigin impairs squamous stratification and apical cell enlargement

Consistent with previous reports, we found that basigin in healthy human corneas localizes to cell membranes of basal cells within the stratified squamous epithelia, as well as superficial cells along the apical region (Figure 1A).[12] To gain insight into the function of basigin in the homeostatic cornea, we took advantage of a human cornea model of squamous epithelial differentiation in which the basigin gene was abrogated using the CRISPR/Cas9 gene-editing system. Use of sgRNA-3 targeting exon 3 of the genomic locus of the human *BSG* gene produced several single cell clones of human corneal epithelial cells presenting undetectable levels of basigin protein (Figure 1B). Transduction with sgRNA-3 in these experiments did not induce unintended editing of the transcription factor *NCOR2*, the only genome-wide off-target site predicted by CAS-OFFinder.

Induction of differentiation in human models of corneal epithelium is associated with stratification and the appearance of flattened squamous cells with increased surface heterogeneity.[23,24] Histological analysis revealed that induction of differentiation in control cells resulted in the formation of stratified cultures with 2–4 cell layers and large, flattened superficial cells (Figure 2A). On the other

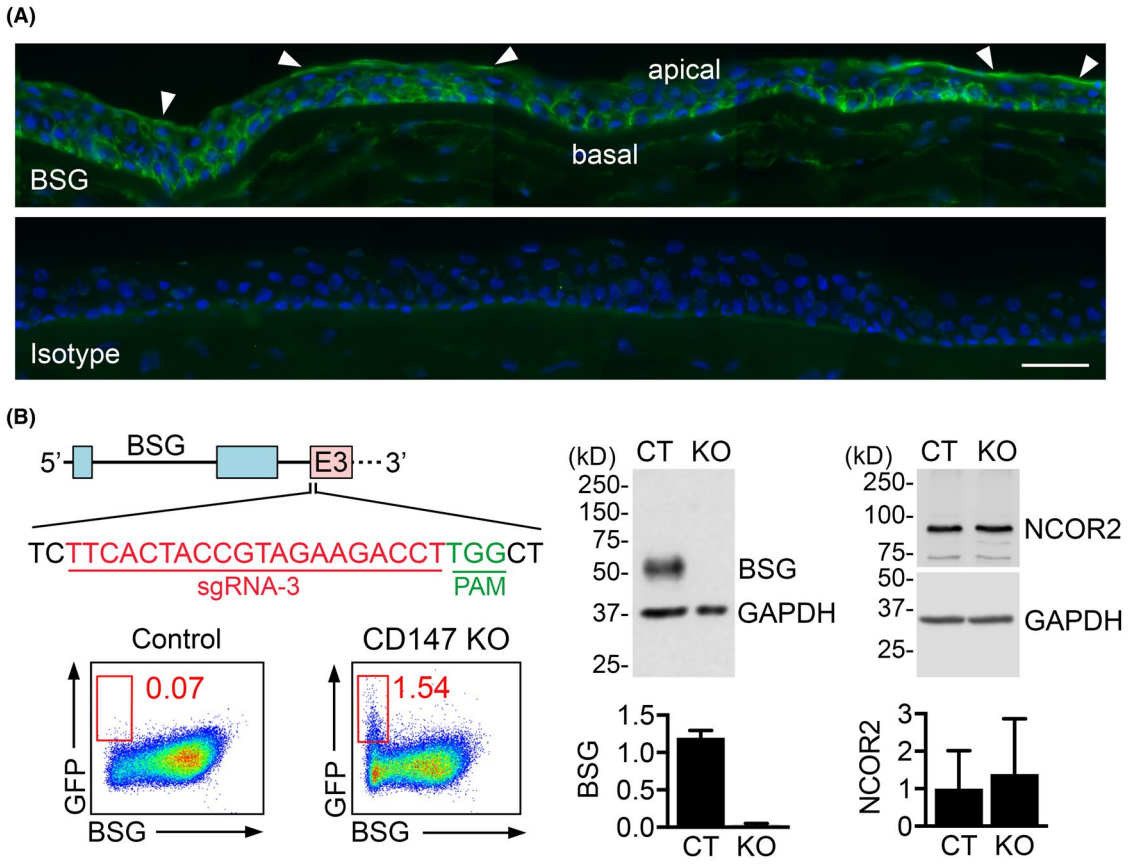

FIGURE 1 CRISPR/Cas9 genome editing efficiently blocks basigin biosynthesis in human corneal epithelial cells. (A) Immunofluorescence micrographs of healthy human corneal epithelial tissue stained with anti-basigin antibody or isotype control. The arrowheads indicate apical localization of basigin. DAPI was used for nuclear staining (blue). (B) Schematic representation of the first three intron-exon organization of the *BSG* gene and location of the sgRNA-3 target site. The target sequence of sgRNA-3 is shown in red and the PAM is shown in green. Subpopulations of GFP^+BSG^- cells were separated by cell sorting. Lysates derived from basigin knockout single cell clones (KO) and noninfected controls (CT) were analyzed by immunoblotting using antibodies against the indicated proteins (n= 3–5 independent clones). Representative blots are shown on top, and quantification of band intensity relative to GAPDH is shown below. Data are expressed as mean ± SD.

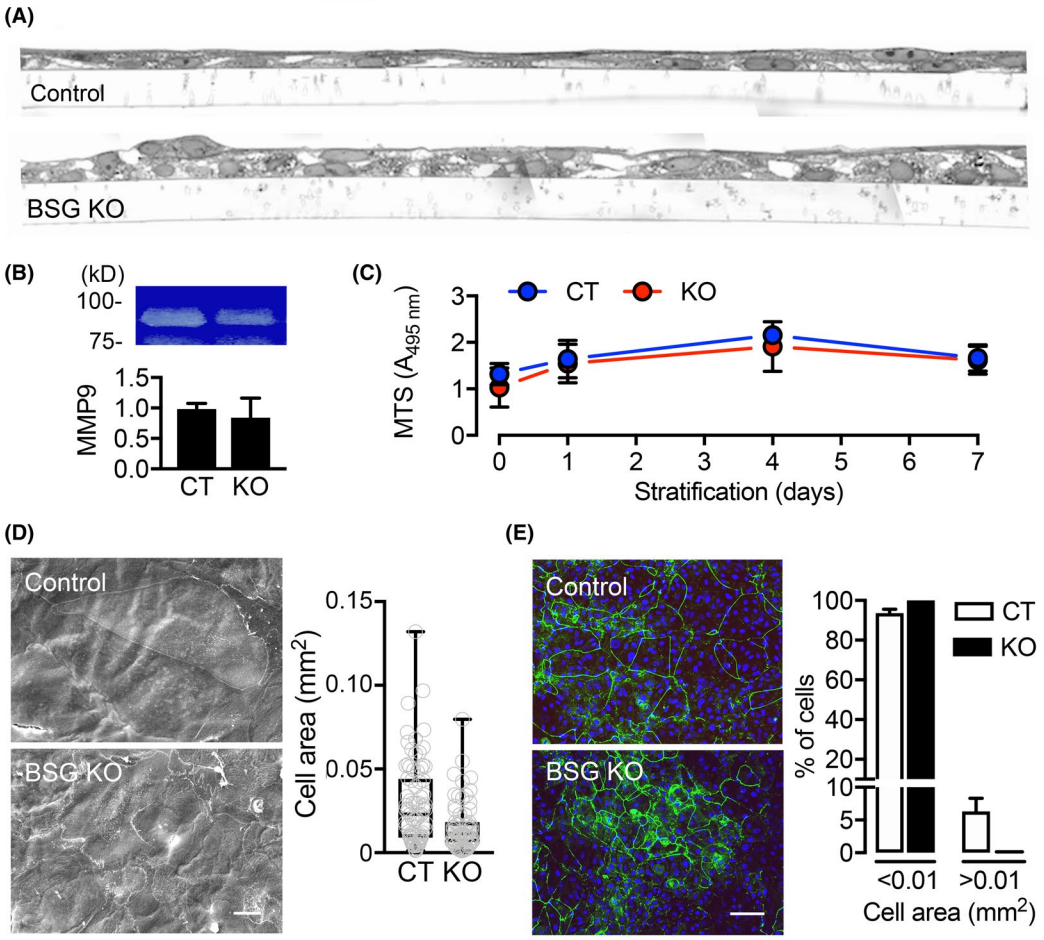

FIGURE 2 Loss of basigin impairs squamous stratification and apical cell enlargement. (A) Toluidine blue-stained semi-thin sections of basigin knockout (KO) and control (CT) cell cultures grown on Transwell inserts. (B) Gelatin zymography of cell culture media (n = 3 independent experiments). A representative image is shown on top, and quantification of band intensity is shown below. (C) The number of viable cells in each culture at different time points during stratification was determined by MTS assay (n = 3 independent experiments). (D) Scanning electron microscopy images of the apical surface of basigin KO and control cell cultures. The images were recorded at 500× magnification. Surface area was measured in approximately 70 cells derived from the examination of 11–12 scans per condition. (E) Immunofluorescence detection of ZO-1 staining at cell borders. Cell area in each image was outlined using ZO-1 staining and quantified using ImageJ software. Surface area was measured in approximately 150 cells per condition from eight images corresponding to three different experiments. DAPI was used for nuclear staining (blue). Data are expressed as mean ±SD. The box-and-whisker plots show the 25th and 75th percentiles (boxes), the median, and the minimum and maximum data values (whiskers). Scale bars: 20 μm (D); 100 μm (E).

hand, stratified cultures null for basigin underwent morphological changes with cells rounding up at the apical cell layer. Analyses of culture supernatants by gelatin zymography revealed no significant changes in the levels of MMP9 produced by the basigin null cultures (Figure 2B), suggesting that lack of proper squamous stratification in these cultures is independent of basigin-mediated matrix metalloproteinase activity. Similarly, we found no differences in proliferative activity that could account for the abnormal appearance of the basigin null cultures (Figure 2C).

In subsequent experiments, we used scanning electron microscopy to gain insight into the surface morphology of apical cells in control and basigin null cultures. Although there was no apparent difference in plasma membrane specializations among these conditions, we found that cultures lacking basigin had a scarce number of cells presenting large surface apical areas (Figure 2D). This finding was further confirmed by immunofluorescence microscopy using a monoclonal antibody directed against ZO-1, a junctional protein present at the cell border. Analysis of cell outlines demonstrated an aberrant distribution of this antibody in the absence of basigin, with cultures lacking squamous cells with large apical surfaces (i.e., those with areas greater than 0.01 mm^2) (Figure 2E).

3.2 | Basigin promotes terminal differentiation of human corneal epithelial cells

To better understand how basigin influences the morphological appearance of human corneal epithelial cells, we evaluated the expression of upstream transcription factors known to regulate terminal epithelial differentiation. We found that the expression of SPDEF, a transcription factor involved in the control of mucin production in mucosal epithelia,[25] was markedly reduced in basigin null cultures (Figure 3A). The influence of basigin on the transcription machinery responsible for terminal differentiation appeared to be selective, since basigin abrogation did not significantly alter the expression levels of KLF4 and ELF3, two other transcription factors associated with the maturation of epithelial cells.[26]

We next asked whether abrogation of basigin in human corneal epithelial cells would alter the expression of well-established markers of terminal differentiation. Toward this purpose, we report here the synthesis and distribution of MUC16, a large transmembrane mucin markedly induced by SPDEF[25] and associated with forming a transcellular barrier in the cornea.[27,28] MUC16 is prevalent on plasma membranes of apical cells in the human cornea, but not in other species such as mouse or rat, which likely reflects an adaptation to different environments.[29] Immunofluorescence microscopy revealed that stratified cultures had a mosaic pattern of MUC16 antibody binding similar to that found in normal human tissue (Figure 3B).[30] On the other hand, cell cultures lacking basigin failed to produce squamous cells expressing MUC16 on their apical surfaces. Downregulation of MUC16 in these cells was further confirmed by immunoblotting (Figure 3C). Interestingly, we did not observe changes in MUC1, the other major mucin expressed in cornea and whose expression appears to antagonize the barrier function of MUC16.[31]

In additional experiments, we also found that lack of basigin led to a significant reduction in the protein levels of galectin-3, a carbohydrate-binding protein that contributes to the glycocalyx barrier through interaction with mucins[32,33] and involucrin, a transglutaminase substrate responsible for the formation of the cell envelope in terminally differentiated stratified squamous epithelia[34] (Figure 3D).

3.3 | Homeostatic basigin expression contributes to maintain barrier function

To better understand how the loss of basigin affects the integrity of terminally differentiated squamous cells, we performed a PCR array targeting the expression of 84 genes involved in epithelial cell polarity and the biogenesis of components of the junctional complex. Epithelial attachment structures serve not only as a crucial component of the mucosal barrier, but also transmit signals that regulate cell proliferation, migration, and survival.[35,36] A direct comparison of the relative expression levels in control cell cultures revealed that the most highly expressed genes included the Rho family of small GTPases, RAC1, RHOA, and CDC42, which are members of the G protein superfamily involved in actin dynamics (Figure 4A, Supplemental Table S2). Other genes prevalently expressed in the human model of squamous stratification were associated with establishing proper cytoskeletal architecture (e.g., actinin and catenins) and signal transduction.

Eight genes were found to be at least tenfold regulated in cultures lacking *BSG* gene expression (Figure 4B). Of these, six genes were downregulated and two upregulated. Downregulation occurred in genes necessary for the stabilization of the tight junction (*zonula occludens*) and included occludin (*OCLN*) and members of the claudin family (*CLDN4*, *CLDN8*, *CLDN9*, and *CLDN17*). One gene encoding a protein mediating intercellular adhesion, ICAM1, was also downregulated. Conversely, loss of basigin resulted in upregulation of two genes encoding the junctional adhesion proteins JAM2 and JAM3, which are specifically enriched at tight junctions. We next focused on occludin since this protein provides structural integrity to epithelial tissues and restricts the paracellular transport pathway.[37] Further, the finding that *OCLN* was downregulated in cultures lacking basigin seemed counterintuitive, since induction of basigin in human corneal epithelial cells has been associated with the proteolytic degradation of occludin and the formation of a dysfunctional epithelial barrier.[13] Consistent with our PCR array data, we found that the protein levels of occludin were significantly downregulated in cell cultures lacking basigin expression (Figure 4C). As shown by immunofluorescence microscopy, these cells lacked the apical staining of occludin along the cell borders present in control cells (Figure 4D). Hence, these results implicate basigin as having dual effects on occludin, acting as an enhancer at the transcriptional level during homeostatic conditions and prompting its proteolytic degradation during pathological states.

The impairment of MUC16 expression in the glycocalyx, as well as the downregulation of genes necessary for the stabilization of tight junctions, led us to evaluate the functional implications of basigin loss to both the transcellular and paracellular epithelial barriers. Rose bengal is a topical ophthalmic dye used to assess damage of the ocular surface epithelial glycocalyx.[38] In our experiments, we found that rose bengal was excluded from

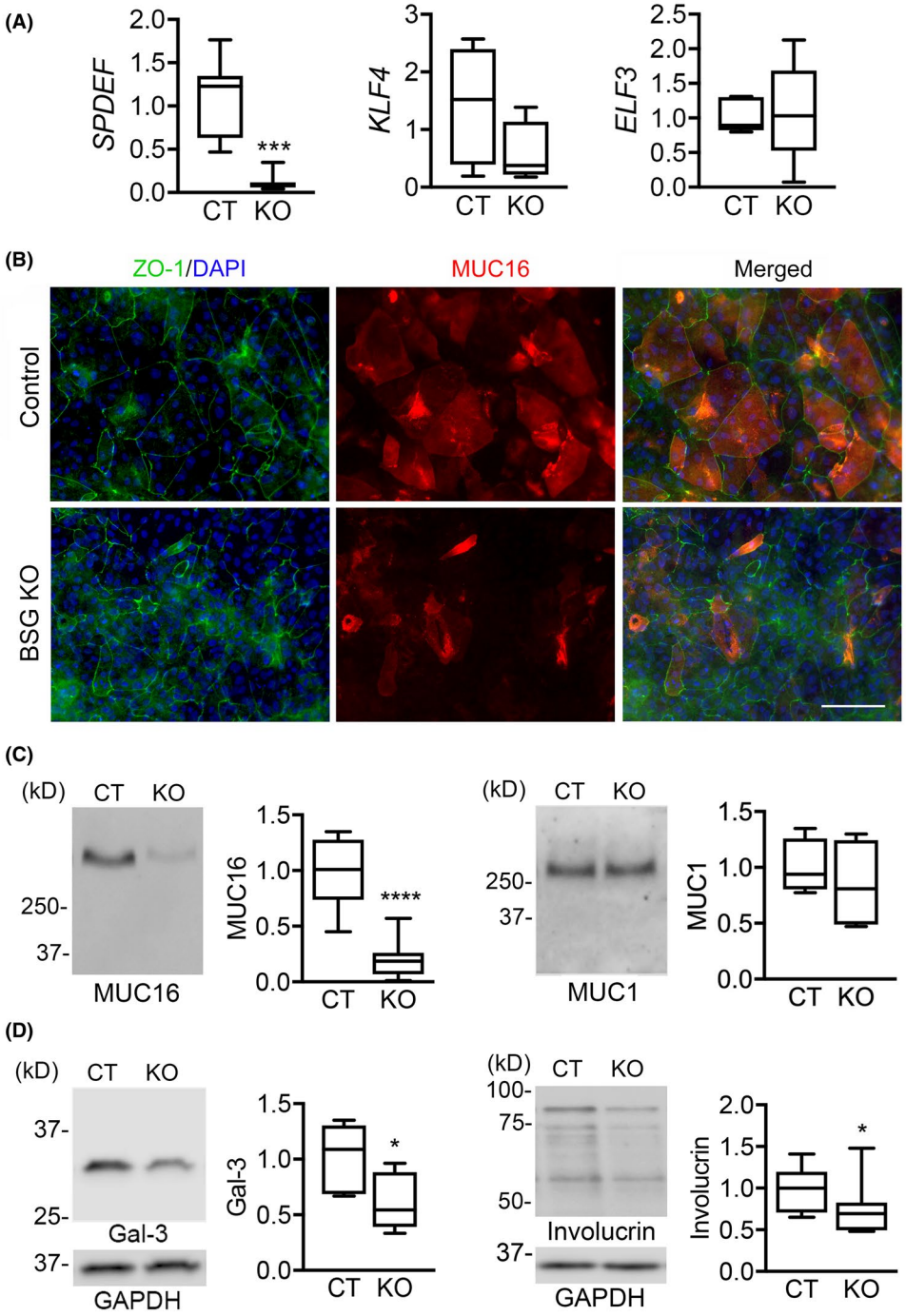

FIGURE 3 Basigin promotes terminal differentiation of human corneal epithelial cells. (A) Gene expression levels of *SPDEF*, *KLF4*, and *ELF3* as determined by qPCR in basigin knockout (KO) and control (CT) cell cultures. The expression of genes was normalized with the $\Delta\Delta C_T$ method. (B) Immunofluorescence colocalization of ZO-1 and MUC16 in basigin knockout and control cell cultures. DAPI was used for nuclear staining (blue). (C and D) Lysates derived from basigin KO and control cell cultures were analyzed by immunoblotting using antibodies against the indicated proteins (n= 4–6 independent experiments). Representative blots are shown to the left, and quantification of band intensity is shown to the right. The box-and-whisker plots show the 25th and 75th percentiles (boxes), the median, and the minimum and maximum data values (whiskers). Significance was determined using the Mann–Whitney *U* test. *, $p < 0.05$; ***, $p < 0.001$; ****, $p < 0.0001$. Scale bar: 100 μm.

islands of stratified cells in control cultures but penetrated to a large extent into cultures lacking basigin expression (Figure 4E). Likewise, abrogation of basigin was associated with an increase in tight junction permeability across the epithelial cultures, as evidenced by a significant reduction in transepithelial electrical resistance (Figure 4F), indicating that basigin is integral to the normal functioning of the human corneal epithelium.

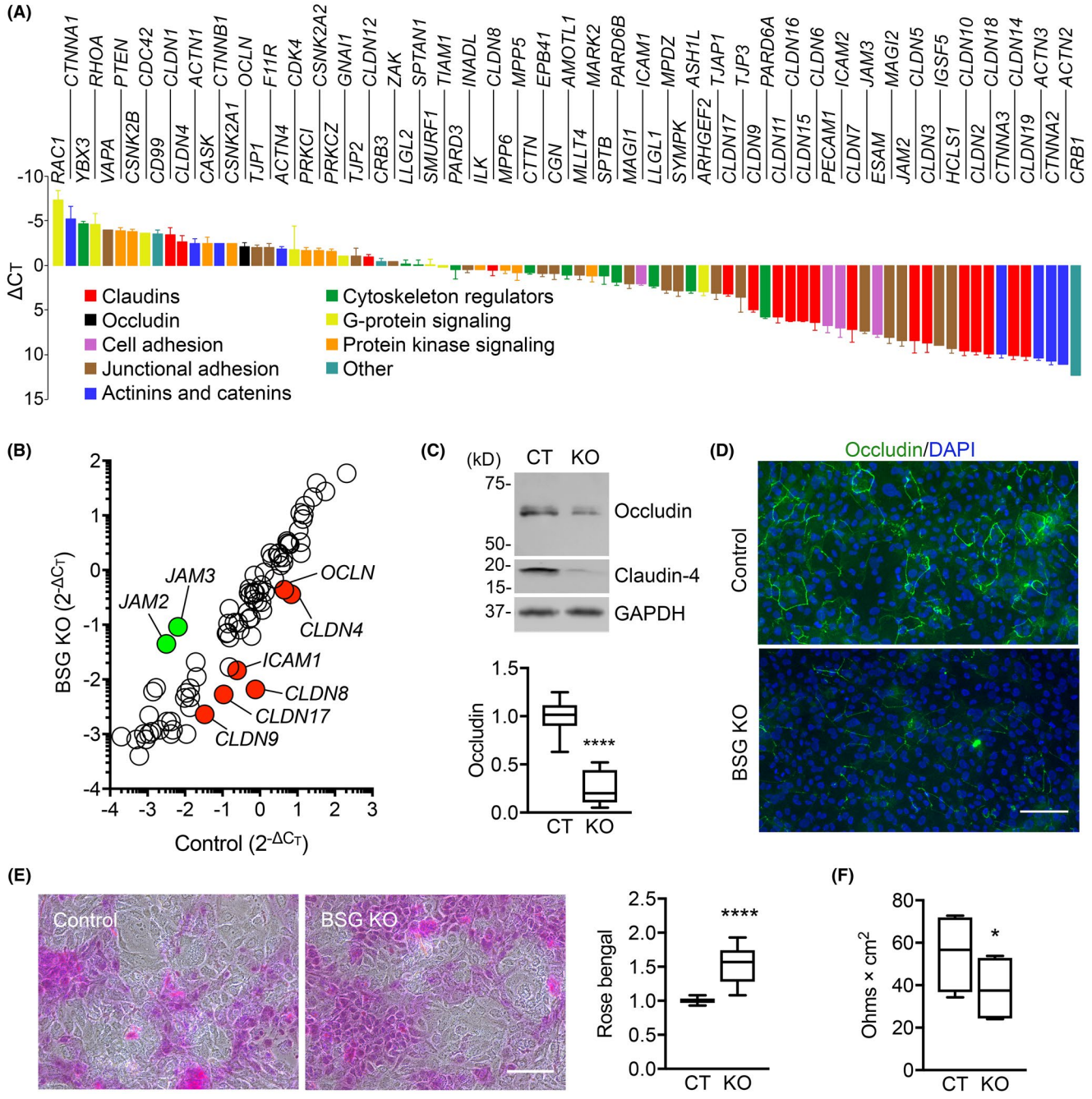

FIGURE 4 Homeostatic basigin expression contributes to maintain barrier function. (A) Relative transcript abundance of genes encoding proteins involved in epithelial cell polarity and the biogenesis of components of the junctional complex in control cultures of human corneal epithelial cells. The expression of genes was determined using a human tight junction PCR array and normalized with the ΔC_T method. (B) Scatterplot comparing the expression of genes in basigin knockout (KO) and control (CT) cell cultures. The green and red dots indicate at least tenfold up- or downregulation, respectively, compared with control. The array was repeated twice with independently isolated RNA. (C) Lysates derived from basigin KO and control cell cultures were analyzed by immunoblotting using antibodies against occludin and claudin-4, the two most highly expressed tight junction components whose transcription was reduced in KO cells (n= 4 independent experiments). Representative blots are shown on top, and quantification of band intensity of occludin relative to GAPDH is shown below. (D) Immunofluorescence detection of occludin staining at cell borders. DAPI was used for nuclear staining (blue). (E) Glycocalyx barrier function was determined by the rose bengal penetration assay. Representative rose bengal images are presented. (F) Barrier function as measured by transepithelial electrical resistance. Data in (A) are expressed as mean ± SD. The box-and-whisker plots show the 25th and 75th percentiles (boxes), the median, and the minimum and maximum data values (whiskers). Significance was determined using the Student's *t*-test (C and F) or the Mann–Whitney *U* test (E). *, $p < 0.05$; ****, $p < 0.0001$. Scale bars: 100 μm.

4 | DISCUSSION

The presence of a nonkeratinized stratified squamous epithelium is highly beneficial to organs that are in close contact with the external environment and regularly exposed to physical abrasion. Identifying the mechanisms that sustain the proper formation and maintenance of this kind of epithelium is critical to reduce the morbidity associated with loss of barrier function.[39,40] In the human cornea, high basigin expression has been observed in pathological conditions where there is aberrant expression of proteolytic enzymes, such as ulceration, fibrosis, and dry eye. These observations have led to recent attempts to pharmaceutically block basigin function.[41] To better understand the role of basigin at the ocular surface, we generated an in vitro human model of squamous cell differentiation where basigin expression was abrogated using a CRISPR/Cas9 genome editing approach. Our results provide compelling evidence that blocking the physiological expression of basigin has deleterious effects on the structural integrity and barrier function of squamous epithelial cells.

This study raises important questions regarding the dual role that basigin exhibits in promoting the degradation or, conversely, the expression of components of the epithelial junction within the same organ. Induction of MMP activity following basigin overexpression is commonly observed in a variety of physiological and pathological conditions that require remodeling such as development, tissue repair, and cancer.[42] The mechanisms regulating basigin-mediated MMP activity are multiple and mostly dependent on the glycosylation status of basigin as well as its homo-oligomerization and heterophilic interactions with other proteins.[43] In cornea, interaction of basigin with the carbohydrate-binding protein galectin-3 results in the MMP-dependent loss of occludin at the tight junction and the disruption of cell–cell contacts.[44] Likewise, increased expression of basigin has been associated with the MMP-mediated cleavage of occludin and loss of barrier function in a model of dry eye disease.[13] These findings are in apparent contrast with the current study showing that basigin is necessary to support the expression and cellular distribution of occludin at cell boundaries in corneal epithelium.

We hypothesize that differences in basigin expression, glycosylation, or ability to multimerize between homeostatic conditions and conditions that require extensive tissue remodeling are responsible for the unique functions of basigin in mediating junctional stability or degradation. Basigin biosynthesis and activation are tightly regulated by complex mechanisms that include cytokines, growth factors, and cellular interactions.[42] In cornea, basigin activation occurs when epithelial cells become in direct contact with neighboring fibroblasts in the underlying stroma following injury.[12] Also, it is known that expression of the basigin partner, galectin-3, in cornea is lower under normal conditions compared to that observed in ulcerated or wounded tissues.[15,45] Therefore, it is feasible to speculate that unique cellular distribution and low levels of basigin and its interacting proteins under homeostatic conditions are insufficient to trigger basigin activation and, consequently, promote MMP expression and loss of barrier function. This hypothesis is consistent with the data indicating that basigin does not play a role in modulating MMP9 activity in our model system of normal squamous differentiation. It is worth noting, however, that the apical corneal epithelium of $Bsg^{-/-}$ mice shows a marked alteration in occludin immunostaining, which appears as long and thick lines compared to the punctate staining observed in wild type controls.[13] Yet, it is unclear from this study whether this observation implies an alteration in occludin protein levels, is linked to abnormal MMP activity in the cornea or has functional consequences to the barrier function of the epithelium. It is also important to keep in mind that some of the actions of basigin could be species specific and be dependent on the model system being studied.

Our findings indicate that homeostatic expression of basigin sustains the transcription of occludin and other components of the tight junction. Yet, the mechanism that contribute to this type of regulation remains unknown. There is no evidence suggesting that basigin contains intrinsic motifs responsible for signal transduction, despite the myriad of signaling events attributed to basigin.[10] It is likely that basigin regulates the expression of components of the tight junction through an indirect mechanism. Previous studies in cancer have shown that basigin trafficking and surface interaction with other proteins modulates cell behavior and signaling.[46,47] An example is the small GTPase Arf6, which regulates the endocytic recycling of basigin in hepatocellular carcinoma cells. Disruption of Arf6-mediated basigin trafficking has been shown to reduce cell adhesion and to disrupt tight junction formation.[48] Similar results have been obtained in immune cells, where the dynamic interaction between basigin and its partners leads to a plethora of phosphorylation events involved in biological processes such as cytoskeletal activity and protein modification.[49] Questions remain as to the trafficking dynamics and protein interactions that regulate basigin activity in human corneal epithelial cells. Fortunately, the use of CRISPR/Cas9 gene-editing technology has proven to be a valuable tool to answer these questions going forward.

ACKNOWLEDGMENTS

The authors thank Dr. Ula Jurkunas at the Massachusetts Eye and Ear Infirmary for the collection of discarded human

corneal tissue and Dr. James Jester at the Gavin Herbert Eye Institute for providing the hTCEpi human corneal epithelial cell line. The authors would also like to thank Philip Seifert and Ann Tisdale for their expert support with electron microscopy.

CONFLICT OF INTEREST

The authors declare no conflict of interest with the contents of this article.

AUTHOR CONTRIBUTIONS

A. M. Woodward, M. N. Feeley, and P. Argüeso designed research; A. M. Woodward, M. N. Feeley, and J. Rinaldi performed research; M. N. Feeley created new knockout cell line; A. M. Woodward and P. Argüeso analyzed data; A. M. Woodward and P. Argüeso wrote the paper.

ORCID

Pablo Argüeso https://orcid.org/0000-0001-7321-9503

REFERENCES

1. Gipson IK, Spurr-Michaud SJ, Tisdale AS, Kublin C, Cintron C, Keutmann H. Stratified squamous epithelia produce mucin-like glycoproteins. *Tissue Cell*. 1995;27:397-404.
2. Knust E. Regulation of epithelial cell shape and polarity by cell-cell adhesion (Review). *Mol Membr Biol*. 2002;19:113-120.
3. France MM, Turner JR. The mucosal barrier at a glance. *J Cell Sci*. 2017;130:307-314.
4. Iacono KT, Brown AL, Greene MI, Saouaf SJ. CD147 immunoglobulin superfamily receptor function and role in pathology. *Exp Mol Pathol*. 2007;83:283-295.
5. Weidle UH, Scheuer W, Eggle D, Klostermann S, Stockinger H. Cancer-related issues of CD147. *Cancer Genomics Proteomics*. 2010;7:157-169.
6. Muramatsu T. Basigin (CD147), a multifunctional transmembrane glycoprotein with various binding partners. *J Biochem*. 2016;159:481-490.
7. Pushkarsky T, Zybarth G, Dubrovsky L, et al. CD147 facilitates HIV-1 infection by interacting with virus-associated cyclophilin A. *Proc Natl Acad Sci U S A*. 2001;98:6360-6365.
8. Xia P, Dubrovska A. Tumor markers as an entry for SARS-CoV-2 infection? *FEBS J*. 2020;287:3677-3680.
9. Biswas C. Collagenase stimulation in cocultures of human fibroblasts and human tumor cells. *Cancer Lett*. 1984;24:201-207.
10. Grass GD, Toole BP. How, with whom and when: an overview of CD147-mediated regulatory networks influencing matrix metalloproteinase activity. *Biosci Rep*. 2015;36:e00283.
11. Riethdorf S, Reimers N, Assmann V, et al. High incidence of EMMPRIN expression in human tumors. *Int J Cancer*. 2006;119:1800-1810.
12. Gabison EE, Mourah S, Steinfels E, et al. Differential expression of extracellular matrix metalloproteinase inducer (CD147) in normal and ulcerated corneas: role in epithelio-stromal interactions and matrix metalloproteinase induction. *The American journal of pathology*. 2005;166:209-219.
13. Huet E, Vallee B, Delbe J, et al. EMMPRIN modulates epithelial barrier function through a MMP-mediated occludin cleavage: implications in dry eye disease. *Am J Pathol*. 2011;179:1278-1286.
14. Seppala HP, Maatta M, Rautia M, et al. EMMPRIN and MMP-1 in keratoconus. *Cornea*. 2006;25:325-330.
15. Cruzat A, Gonzalez-Andrades M, Mauris J, et al. Colocalization of Galectin-3 With CD147 is associated with increased gelatinolytic activity in ulcerating human corneas. *Invest Ophthalmol Vis Sci*. 2018;59:223-230.
16. Asakura T, Yokoyama M, Shiraishi K, Aoki K, Ohkawa K. Chemotherapeutic effect of CD147 antibody-labeled micelles encapsulating doxorubicin conjugate targeting CD147-expressing carcinoma cells. *Anticancer Res*. 2018;38:1311-1316.
17. Robertson DM, Li L, Fisher S, et al. Characterization of growth and differentiation in a telomerase-immortalized human corneal epithelial cell line. *Invest Ophthalmol Vis Sci*. 2005;46:470-478.
18. Walter DM, Venancio OS, Buza EL, et al. Systematic in vivo inactivation of chromatin-regulating enzymes identifies Setd2 as a potent tumor suppressor in lung adenocarcinoma. *Cancer Res*. 2017;77:1719-1729.
19. Tang Y, Garson K, Li L, Vanderhyden BC. Optimization of lentiviral vector production using polyethylenimine-mediated transfection. *Oncol Letters*. 2015;9:55-62.
20. Bae S, Park J, Kim JS. Cas-OFFinder: a fast and versatile algorithm that searches for potential off-target sites of Cas9 RNA-guided endonucleases. *Bioinformatics*. 2014;30:1473-1475.
21. Nakarai C, Osawa K, Matsubara N, et al. Significance of ELF3 mRNA expression for detection of lymph node metastases of colorectal cancer. *Anticancer Res*. 2012;32:3753-3758.
22. Argueso P, Gipson IK. Assessing mucin expression and function in human ocular surface epithelia in vivo and in vitro. *Methods Mol Biol*. 2012;842:313-325.
23. Yanez-Soto B, Leonard BC, Raghunathan VK, Abbott NL, Murphy CJ. Effect of stratification on surface properties of corneal epithelial cells. *Invest Ophthalmol Vis Sci*. 2015;56:8340-8348.
24. Gipson IK, Spurr-Michaud S, Argueso P, Tisdale A, Ng TF, Russo CL. Mucin gene expression in immortalized human corneal-limbal and conjunctival epithelial cell lines. *Invest Ophthalmol Vis Sci*. 2003;44:2496-2506.
25. Chen G, Korfhagen TR, Xu Y, et al. SPDEF is required for mouse pulmonary goblet cell differentiation and regulates a network of genes associated with mucus production. *J Clin Invest*. 2009;119:2914-2924.
26. Sancho E, Batlle E, Clevers H. Live and let die in the intestinal epithelium. *Curr Opin Cell Biol*. 2003;15:763-770.
27. Argueso P, Spurr-Michaud S, Russo CL, Tisdale A, Gipson IK. MUC16 mucin is expressed by the human ocular surface epithelia and carries the H185 carbohydrate epitope. *Invest Ophthalmol Vis Sci*. 2003;44:2487-2495.
28. Blalock TD, Spurr-Michaud SJ, Tisdale AS, et al. Functions of MUC16 in corneal epithelial cells. *Invest Ophthalmol Vis Sci*. 2007;48:4509-4518.
29. Fini ME, Jeong S, Gong H, et al. Membrane-associated mucins of the ocular surface: new genes, new protein functions and new biological roles in human and mouse. *Prog Retin Eye Res*. 2020;75:100777.
30. Gipson IK, Argueso P. Role of mucins in the function of the corneal and conjunctival epithelia. *Int Rev Cytol*. 2003;231:1-49.
31. Gipson IK, Spurr-Michaud S, Tisdale A, Menon BB. Comparison of the transmembrane mucins MUC1 and MUC16 in epithelial barrier function. *PLoS One*. 2014;9:e100393.

32. Argueso P, Guzman-Aranguez A, Mantelli F, Cao Z, Ricciuto J, Panjwani N. Association of cell surface mucins with galectin-3 contributes to the ocular surface epithelial barrier. *J Biol Chem*. 2009;284:23037-23045.
33. Taniguchi T, Woodward AM, Magnelli P, et al. N-Glycosylation affects the stability and barrier function of the MUC16 mucin. *J Biol Chem*. 2017;292:11079-11090.
34. Steinert PM, Marekov LN. Initiation of assembly of the cell envelope barrier structure of stratified squamous epithelia. *Mol Biol Cell*. 1999;10:4247-4261.
35. Zihni C, Balda MS, Matter K. Signalling at tight junctions during epithelial differentiation and microbial pathogenesis. *J Cell Sci*. 2014;127:3401-3413.
36. Miyoshi J, Takai Y. Molecular perspective on tight-junction assembly and epithelial polarity. *Adv Drug Deliv Rev*. 2005;57:815-855.
37. Cummins PM. Occludin: one protein, many forms. *Mol Cell Biol*. 2012;32:242-250.
38. Bron AJ, Argueso P, Irkec M, Bright FV. Clinical staining of the ocular surface: mechanisms and interpretations. *Prog Retin Eye Res*. 2015;44:36-61.
39. Blevins CH, Iyer PG, Vela MF, Katzka DA. The esophageal epithelial barrier in health and disease. *Clin Gastroenterol Hepatol*. 2018;16:608-617.
40. Mantelli F, Mauris J, Argueso P. The ocular surface epithelial barrier and other mechanisms of mucosal protection: from allergy to infectious diseases. *Curr Opin Allergy Clin Immunol*. 2013;13:563-568.
41. Joung C, Noh H, Jung J, et al. A novel CD147 inhibitor, SP-8356, attenuates pathological fibrosis in alkali-burned rat cornea. *Int J Mol Sci*. 2020;21(8):2990.
42. Gabison EE, Hoang-Xuan T, Mauviel A, Menashi S. EMMPRIN/CD147, an MMP modulator in cancer, development and tissue repair. *Biochimie*. 2005;87:361-368.
43. Huang W, Luo WJ, Zhu P, et al. Modulation of CD147-induced matrix metalloproteinase activity: role of CD147 N-glycosylation. *Biochem J*. 2013;449:437-448.
44. Mauris J, Woodward AM, Cao Z, Panjwani N, Argueso P. Molecular basis for MMP9 induction and disruption of epithelial cell-cell contacts by galectin-3. *J Cell Sci*. 2014;127:3141-3148.
45. Cao Z, Said N, Amin S, et al. Galectins-3 and -7, but not galectin-1, play a role in re-epithelialization of wounds. *J Biol Chem*. 2002;277:42299-42305.
46. Qi S, Su L, Li J, et al. YIPF2 is a novel Rab-GDF that enhances HCC malignant phenotypes by facilitating CD147 endocytic recycle. *Cell Death Dis*. 2019;10:462.
47. Wu B, Wang Y, Yang XM, et al. Basigin-mediated redistribution of CD98 promotes cell spreading and tumorigenicity in hepatocellular carcinoma. *J Exp Clin Cancer Res*. 2015;34:110.
48. Qi S, Su L, Li J, et al. Arf6-driven endocytic recycling of CD147 determines HCC malignant phenotypes. *J Exp Clin Cancer Res*. 2019;38:471.
49. Supper V, Hartl I, Boulegue C, Ohradanova-Repic A, Stockinger H. Dynamic interaction- and phospho-proteomics reveal Lck as a major signaling hub of CD147 in T cells. *J Immunol*. 2017;198:2468-2478.

SUPPORTING INFORMATION

Additional supporting information may be found in the online version of the article at the publisher's website.

How to cite this article: Woodward AM, Feeley MN, Rinaldi J, Argüeso P. CRISPR/Cas9 genome editing reveals an essential role for basigin in maintaining a nonkeratinized squamous epithelium in cornea. *FASEB BioAdvances*. 2021;3:897–908. https://doi.org/10.1096/fba.2021-00067